Atmos. Chem. Phys., 11, 11511–11519, 2011
www.atmos-chem-phys.net/11/11511/2011/
doi:10.5194/acp-11-11511-2011

Atmospheric Chemistry and Physics

Fast sulfur dioxide measurements correlated with cloud condensation nuclei spectra in the marine boundary layer

D. C. Thornton[1], **A. R. Bandy**[1], **and J. G. Hudson**[2]

[1]Department of Chemistry, Drexel University, Philadelphia, PA, USA
[2]Desert Research Institute, Nevada System of Higher Education, Reno, NV, USA

Received: 2 May 2011 – Published in Atmos. Chem. Phys. Discuss.: 17 May 2011
Revised: 26 October 2011 – Accepted: 9 November 2011 – Published: 21 November 2011

Abstract. During the Rain in (shallow) Cumulus over the Ocean (RICO) project simultaneous high rate sulfur dioxide (SO_2) measurements and cloud condensation nuclei (CCN) spectra were made for the first time. For research flight 14 (14 January 2005) the convective boundary layer was impacted by precipitation and ship plumes for much of the midday period but not in the late afternoon. Number densities of accumulation mode aerosols (0.14 to 0.2 µm diameter) were a factor of two greater in the later period while CCN were 35 % to 80 % greater for aerosols that activate at supersaturations >0.1 %. Linear correlations of SO_2 and CCN were found for SO_2 concentrations ranging from 20 to 600 parts-per-trillion (pptv). The greatest sensitivities were for SO_2 and CCN that activate at supersaturations >0.1 % for both clean and polluted air. In a region unaffected by pollution SO_2 was linearly correlated only with CCN at >0.2 % supersaturation. These correlations imply that the smallest CCN may be activated by SO_2 through heterogeneous conversion. Evidence for entrainment of CCN from the cloud layer into the CBL was found.

1 Introduction

The Rain in (shallow) Cumulus over the Ocean (RICO) project was an intensive study of shallow cumulus clouds within the trade wind (TW) inversion (Rauber et al., 2007b). The field program was designed so that continuous radar measurements to detect precipitation were combined with intensive physical and chemical measurements obtained with several aircraft and a ship operating within the radar domain and primarily upwind of the radar site. A primary goal of RICO was to understand the conditions that exist at the onset of precipitation in the shallow cumulus clouds of the TW regime.

Several studies have considered factors that could be dominant in forming cloud drops during RICO: low level wind speeds and aerosol size distributions (Colon-Robles et al., 2006), cloud condensation nuclei (CCN) and updraft velocities (Hudson and Mishra, 2007); (Hudson et al., 2009), giant and ultragiant CCN (Arthur et al., 2010; Colon-Robles et al., 2006; Lowenstein et al., 2010; Reiche and Lasher-Trapp, 2010; Hudson et al., 2011) and the submicron sized aerosols (Lowenstein et al., 2010). Gerber et al. (2008) point out these studies inferred the importance of subcloud aerosol measurements and near cloud base concentrations of droplets but neglected processes in the upper portions of the clouds including entrainment of environmental air above the convective boundary layer (CBL).

This study presents a more detailed investigation of the subcloud aerosol distributions and their relationship to sulfur dioxide (SO_2). SO_2 is a precursor to the formation of sulfate aerosols that are considered important in forming and modifying aerosols that could become CCN as well as modifying the number concentrations and size distributions of cloud droplets. The RICO project was the first time that CCN supersaturation spectra and high rate (25 Hz sampling), continuously calibrated, high sensitivity SO_2 measurements were made simultaneously. In addition, SO_2 measurements were fast enough to estimate its flux to the surface by the eddy correlation technique. SO_2 measurements within clouds were also obtained that can be evaluated with respect to droplet concentrations.

Research flight 14 (RF14, 14 January 2005) of the National Center for Atmospheric Research (NCAR) C-130 was typical of many of the RICO C-130 flights with respect to the SO_2 concentrations. Plumes of SO_2 on the order of tens of km long were often encountered during the first circular

Correspondence to: D. C.Thornton
(dct@drexel.edu)

flight track in the CBL near the surface. The most likely sources of these plumes were ships, which were occasionally observed visually. While RICO was considered "clean" for aerosol concentrations compared to continental or near shore conditions, the SO_2 concentrations were much higher than those encountered in the central Pacific CBL (Thornton et al., 1999; Bandy et al., 1996).

The SO_2 plumes in the CBL during the early part of RF14 were remarkable in their magnitude and areal extent for a region expected to be clean with a long fetch of TW. Peak CBL SO_2 concentrations reached 600 pptv and concentrations >100 pptv were pervasive in the CBL. During flight legs at 800 and 1300 m above sea level (a.s.l.) devoted to in situ sampling of the shallow cumulus clouds within the TW inversion, numerous encounters of $SO_2 > 100$ pptv within the clouds were observed. In contrast, SO_2 concentrations above the CBL outside of clouds, but below the TW inversion, were <35 pptv except for a few short encounters with aircraft exhaust. The descriptions of the SO_2 in clouds are the subject of another paper.

2 Measurements

The suite of chemical measurements for RICO was limited in that the program was devoted to understanding the initiation of precipitation in the warm shallow cumulus clouds. The C-130 chemistry data set, in addition to SO_2, included dimethyl sulfide (DMS), ozone (O_3), water vapor, hydrogen peroxide (H_2O_2), and methyl hydroperoxide (CH_3O_2H). The sampling rates for all these gases were $25\,s^{-1}$ except for the peroxides although detector noise limited DMS data to $1\,s^{-1}$. The C-130 physics data set included CCN spectrometers from Desert Research Institute (DRI) (Hudson and Mishra, 2007; Hudson et al., 2009), the standard set of NCAR atmospheric state measurements, condensation nuclei (CN) counters, probes for aerosols (PCASP-200), cloud droplets (FSSP-100), and hydrometeors (260-X, 2DC, 2DP). Throughout the RICO project the NCAR S-band (10 cm) radar was running nearly continuously, which provided a look at the precipitation conditions upwind in the hours prior to and during the aircraft flights. The full suite of the instruments and measurements employed has been described in a supplement to the RICO overview paper (Rauber et al., 2007a).

The SO_2 measurements during RICO were obtained using an atmospheric pressure ionization mass spectrometer (APIMS) with continuous calibration using isotopically labeled sulfur dioxide ($^{34}SO_2$) added to the sampled air (Thornton et al., 2002). The power of this technique lies not only in the signal calibration but in the continuous indication of the performance of the APIMS in terms of sensitivity and response times under all operating conditions (Bandy et al., 1993). A blank determination was obtained using about 50 cm of 6 mm copper tubing, which removed 500 to 800 pptv SO_2 with a 1/e time of 0.58 s. Sampling at 25 Hz allows determination of SO_2 on a physical scale of 10 m. This is a great advantage for detecting SO_2 at the transitions near the cloud edges as well as variations within clouds related to the physical dynamics of the clouds. In addition, the fast response allowed detection of transients of SO_2 produced by aircraft and ship exhausts.

The typical C-130 flight patterns were divided between circular tracks in the CBL (Table 1) and the free troposphere (FT) regions and directed cloud sampling as frequently as possible. An initial 30 min circular track (FT1) was flown above the TW inversion in the region of interest. During this segment dropsondes were released periodically around the track to give a preview of the TW layer meteorological conditions. After descent to about 90 m a.s.l., a 30 min circular track (SU1, see Table 1) was flown followed by a sub cloud base circle (SC) about 450 m a.s.l. The starting locations of the CBL circles were approximately colocated and flown with opposite rotations. All the circles were advected with the mean wind with respect to the starting location.

Following the CBL circles, 3 to 4 h were devoted to sampling in and around clouds within the TW inversion. Altitudes for cloud sampling were determined by the depth of clouds for that flight with an effort to provide a representative sampling of different levels of cloud development. The remaining flight time was spent by repeating the sub-cloud base circle (SC2), a surface circle (SU2), and ascent to a final circle in the free troposphere (FT2) with dropsondes deployed as before.

3 Discussion

The RICO flight program was designed for a detailed study of clouds and precipitation using in situ measurements and remote sensing of the region defined by the radar domain. This strategy effectively made the experiment an Eulerian one, although each circle in the CBL and the FT was drifted with the wind in a Lagrangian mode. While RICO was not a process study, the 4 to 5 h time step between the initial and ending CBL circles allows some inferences to be made about the chemistry and evolution of aerosols as the day progressed. Given the long upwind fetch in a trade wind region of relative consistency, this may be a good assumption with regard to the chemistry and aerosol physics.

With the RICO domain in the TW regime to the north and east of Antigua and Barbuda, advection of air parcels relatively free of anthropogenic impacts from long range was expected. For RF14 the wind direction near the surface was about 75° at 12 to 16 m s^{-1} throughout the flight, except near the beginning and end positions of SU1 where wind speeds were 8 to 13 m s^{-1}. The cloud layer had winds about 90° about 15 m s^{-1} except near 2 km a.s.l. where the wind speeds were ~13 m s^{-1}. RF 14 had the highest average winds for the RICO program. The first low circles (SU1 and SC1) were

Table 1. Start times of CBL circles for RICO RF14.

SU1	Initial surface circle at 90 m	16:12:19 UTC*
SC1	Initial sub-cloud circle at 450 m	16:49:04 UTC
SU2	Final surface circle at 90 m	21:46:39 UTC
SC2	Final sub-cloud circle at 450 m	21:09:49 UTC

* Local time is UTC-4.

affected by several periods of cooler temperatures due to evaporative cooling of rain (cold pool effect), which also resulted in decreased turbulence indicated by the vertical wind component.

One advantage of the RICO project was that the S-band radar was running nearly continuously throughout the experimental period. In the absence of a Lagrangian mode process study, the radar data provide a look at the precipitation conditions upwind in the hours prior to and during the aircraft flight. To estimate the influence that precipitation may have had on SO_2 and aerosols observed during the low altitude circles, every point along the CBL flight tracks was advected back in time using the u and v component winds for each second along the track to the time of the 0.5° elevation radar scan. A composite of the time series of the advected tracks superimposed on the radar plots can then be viewed to follow the development of potential precipitation impacts.

Inspection of the time series of the back advected aircraft tracks for the SU1 and SC1 showed that the beginning and ending parts of these circles were affected by precipitation for nearly the entire time (1 to 1.5 h) the air parcels were within the radar range. The central portions of these two CBL circles were free of precipitation for the entire time the parcels were within the radar range. It was these central portions of the CBL tracks that had a doubling of the accumulation mode aerosols between the beginning and the end of the flight (Table 3 and Fig. 4). Unfortunately, portions of these central sections were also impacted by the ship plumes for the SU1 and SC1 circles, which limited the data for direct comparisons of SO_2 and aerosols for the entire period. The radar plots and the back advected tracks for the late afternoon did not indicate any precipitation for the SU2 and SC2 circles although the cloud cover was similar to the earlier CBL circles.

3.1 Vertical gradients

A distinguishing feature of the CBL is that scalars are well mixed from near the surface to the top of the layer defined by the turbulence in the CBL. The simplest case is a one layer system like the cloud topped stratocumulus BL. The TW regime can be described as a two layer system where the well mixed CBL is topped by an intermittently mixed layer with clouds extending as far as the TW inversion. Precipitation and the effects of evaporating precipitation (cold pool effect) can disrupt the usually well mixed CBL of the TW regime. The cold pools are marked by decreases in equivalent potential temperature (Θ_e) and decreases in turbulence compared to the warmer CBL air.

RF14 was similar to many RICO flights in the CBL with SO_2 concentrations typical of northern hemisphere marine CBL (Thornton et al., 1993; Tu, 2004) but atypical of a remote TW CBL in the Pacific (Thornton et al., 1999). Although the region appeared free of the impacts of continental sources, numerous ships transited the area (Capaldo et al., 1999) as well as the presence of the R/V *Seward Johnson*, which provided a platform for a cloud radar and a wind profiler. For RF14 this impacted area included the starting and ending portions of the CBL circles (between 61.1° W to 62.1° W and 17.7° N to 18.1° N). During the SU1 circle of RF14 SO_2 concentrations were as high as 597 pptv (Fig. 1) and vertical mixing in the CBL resulted in $SO_2 > 100$ pptv as high as 500 m a.s.l. (Fig. 2). Convection in the CBL also resulted in $SO_2 > 100$ pptv within small cumulus clouds at 800–1300 m a.s.l. This convection of SO_2 occurred over the portion of RF14 where the most precipitation was observed by the S-band radar for the CBL circles.

For the section of the SU1 and SC1 circles where the pollution plumes and precipitation were absent, a vertical gradient was observed with a 27 % decrease in the mean SO_2 from 90 m to 450 m (Table 2). At the same time there was also a marked vertical gradient for the mean DMS with 85 pptv for SU1 and 55 pptv for SC1. Water vapor mixing ratio (MR) and O_3 concentrations showed no gradient within the CBL for this portion of the flight, and there was no apparent cold pool effect in this region for SU1 or SC1. Unfortunately, there was no H_2O_2 data for this period of SU1 to assess the gradient for this soluble gas species. Note that the aircraft vertical profile from 90 m to 470 m took place on the opposite side of the circles, which was where the precipitation had occurred. Based on the vertical wind velocity component and the MR during the climb in altitude, there appeared to be some disturbance to the CBL structure between 250 m and 400 m.

The vertical gradient in CN for this same period had an 11 % decrease between SU1 and SC1 (Table 2). CCN number concentrations had the opposite trend with an increase of 12 % at 1.5 % supersaturation (Fig. 5) with the largest contribution from CCN at supersaturations $\leq$0.1 %. The CCN number concentrations could account for 56 % of CN concentrations for SC1 and for 45 % of CN concentrations for SU1.

For the locations of SU2 and SC2 comparable to areas of SU1 and SC2 free of the pollution and precipitation, there was no vertical gradient in SO_2 but CN had the same 11 % decrease in concentrations with altitude as in the earlier CBL circles. However, the CCN number concentrations decreased with altitude by 6 % at 1.5 % supersaturation but by 14 % at 0.04 % supersaturation with the largest contribution from CCN at supersaturations $\leq$0.1 % (Fig. 5). The CCN

Table 2. NCAR CN number concentrations and SO_2 concentrations for the CBL circles of RICO RF14 without direct effects of ship plumes and precipitation. Measurements of CN and SO_2 sampled at 25 s^{-1} were integrated to 1 s.

		CN (# cm^{-3})		SO_2 (pptv)	
Circle	Time into circle	Mean	Std. dev.	Mean	St. Dev.
SU1	901 to 1200 s	245	5.57	40.4	2.32
SC1	980 to 1200 s	218	6.05	29.2	1.76
SU2	800 to 1100 s	320	6.99	27.6	2.61
SC2	501 to 1100 s	283	5.10	28.5	2.19

concentrations could account for 64 % of CN concentrations for SC2 and 61 % of CN concentrations for SU2. For the accumulation mode and larger aerosols (Fig. 3 and Table 2) there was no vertical gradient for either early or late CBL periods.

There could have been several sources of the observed vertical gradients. SO_2 ranged from 20 to 35 pptv in cloud free air above the CBL (excluding brief encounters with aircraft exhausts). However, dilution of SO_2 in the CBL by entrainment of SO_2 from the cloud layer would have been insufficient to produce the observed decrease in SO_2 in the <1 hr time difference between the SU1 and SC1 measurements. The SO_2 flux estimated by the eddy correlation technique was an upward +0.51 pptv m s^{-1} for this SC1 time period. This segment of SC1 had many more clouds overhead than during SU1. Because CN can be expected to be transported as gases would, loss of SO_2 and CN to the cloud layer would be consistent with the data.

The greater relative decrease for SO_2 compared to CN may indicate that there could be a chemical loss path as well as a transport loss path. The decrease of SO_2 during this portion of SC1 and the increase in CCN may be the result of CCN formation and growth aided by SO_2 oxidation. The primary oxidant for SO_2 was likely H_2O_2, which had concentrations of 800–1000 pptv throughout the CBL for all the RF14 CBL circles, although there was no H_2O_2 data available for the period of SU1 discussed here.

3.2 Time evolution

The small increases in CCN concentrations in the vertical gradients during SC1 relative to SU1 were dwarfed by the much greater CCN concentrations for supersaturations ≥0.2 % (Fig. 5) for both SU2 and SC2 compared to the earlier CBL circles. The increase in CCN in the CBL implies that the higher concentrations of CCN during SU2 and SC2 were a net result of increased production or input with loss mechanisms which were slow, diminished, or absent. The absence of gradients in SO_2, O_3, water vapor MR, and H_2O_2

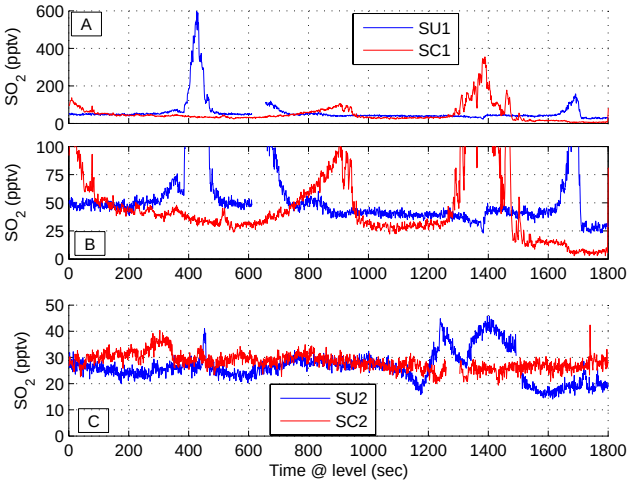

Fig. 1. SO_2 (1 Hz) time series for CBL circles of RICO RF14. Panel **(B)** shows an expanded scale of **(A)**. Times are relative to the start times of circles given in Table 1. The SO_2 peak near 1400 s of SC1 is not the same one as the peak in near 450 s of SU1, which was 40 km downwind at the time of the peak in SC1.

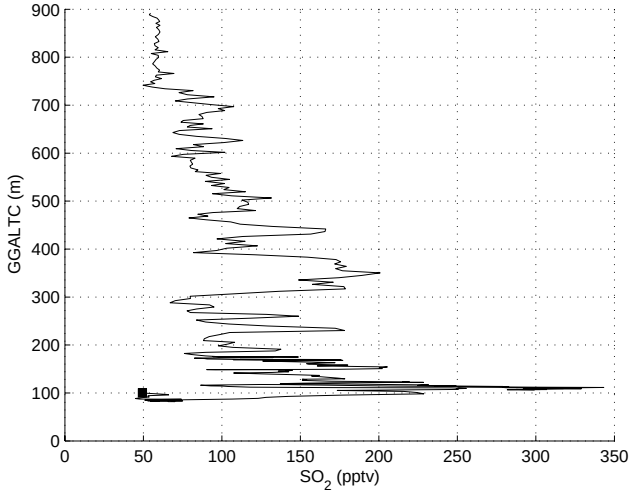

Fig. 2. Portion of the C-130 descent in clear air to the start of the first surface circle (filled square). SO_2 > 100 pptv from probable ship plumes was mixed to 500 m a.s.l. Data obtained at 25 samples s^{-1} were integrated to 1 s^{-1}.

in the CBL for the later circles attest to the stability of the CBL for this period. Under these stable conditions, a major source of CCN production could be entrainment from the cloud layer of small aerosols which were modified by cloud processing, not removed by precipitation, and remained in the cloud layer after clouds had dissipated. The primary loss mechanism for CCN in the CBL is likely to be convection into the cloud layer.

These increases in CCN concentrations appeared to be related to the lack of precipitation (based on the radar scans)

Table 3. Statistics for the PCASP-200 concentrations (# cm^{-3}) for sizes 0.14 to 2.75 µm integrated for 1 s for the precipitation free periods 500 to 1200 s of each circle.

Circle	Mean	Std. Dev.	Std. error of mean
SU1	35.4	7.11	0.27
SU2	69.1	10.5	0.40
SC1	37.5	6.79	0.26
SC2	65.2	9.13	0.34

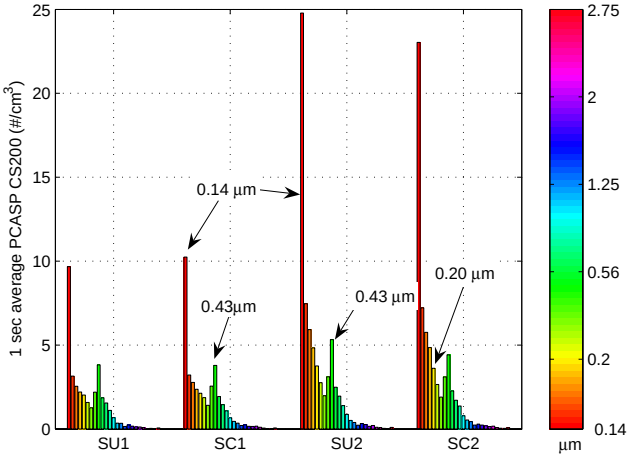

Fig. 3. Size spectra from 10 Hz PCASP-200 integrated over the 500 s to 1200 s portions of the CBL circles of RICO RF14 excluding the periods of precipitation and pollution.

during the hours prior to the measurements. Precipitation averaged over the radar domain during RICO was typically <10 % with an estimate of ∼15 % for RF14 (Rauber et al., 2007b; Snodgrass et al., 2009). In the absence of precipitation it would be possible for entrainment to be a major source of CCN formed in the cloud layer and modified by cloud processing. It is unlikely that the large increase in CCN concentrations was due to any homogeneous or heterogeneous processes in the CBL within the ∼5 h time between SU1 and SU2. Most likely heterogeneous processes over a number of days would have produced this result. The CBL conditions for this portion of RF14 were much more like that observed in the central Pacific trade wind regime where CCN concentrations exceeded 300 cm^{-3} in a CBL with few clouds above and little or no precipitation (Hudson et al., 2009).

In the precipitation free areas the fluxes of SO_2 at 90 m were -0.34 pptv m s^{-1} for SU1 and -0.28 pptv m s^{-1} for SU2, which would contribute a 9 pptv loss of SO_2 to the surface (the sea or aerosols) for the ∼5 h time between SU1 and SU2 for an observed CBL depth of ∼600 m. This difference was nearly equal to the decrease of the mean pollution free SO_2 concentrations from 40 pptv to 29 pptv, respectively, for

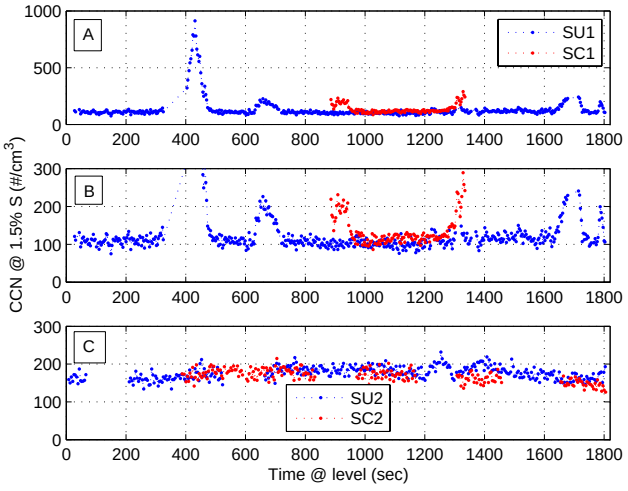

Fig. 4. Cumulative CCN at 1.5 % supersaturation for the CBL circles of RICO RF14 excluding the periods of precipitation. Panel **(B)** shows an expanded scale of **(A)**.

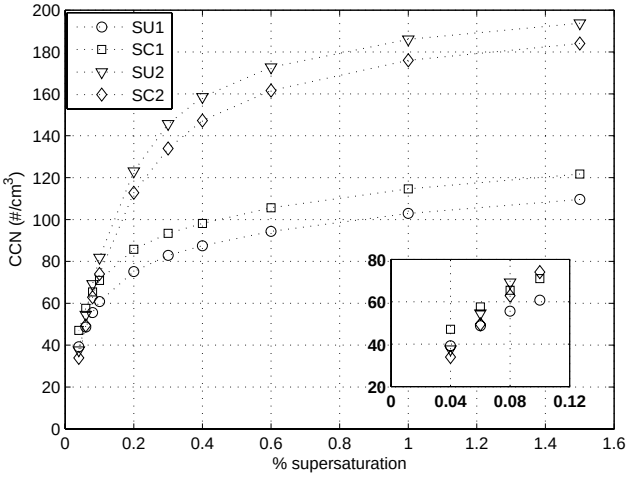

Fig. 5. Mean CCN cumulative concentrations as a function of supersaturation from the four CBL circles for periods free of SO_2 pollution and precipitation.

SU1 and SU2. Over the same time period mean DMS concentrations decreased from 87 pptv for SU1 to 66 pptv during SU2. With a unit production efficiency of SO_2 from DMS, an upper limit to the increase in SO_2 would have been 21 pptv assuming upwind sources of DMS and the CBL conditions were similar throughout the time period. A lower limit for a DMS source of SO_2 could be as low as 15 pptv of ∼0.7 (Bandy et al., 1996; Davis et al., 1999). Consequently, DMS could have provided a source of SO_2 that could balance SO_2 losses to convection and reactions that could support the increased concentrations of CCN at supersaturations of 0.2 % to 0.6 %. While the details for the homogenous formation and oxidation of DMS to SO_2 to sulfuric acid have been

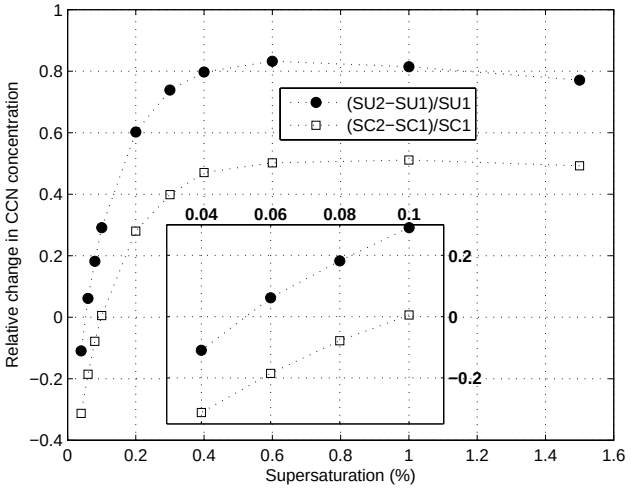

Fig. 6. Change in the cumulative CCN means for the late afternoon circles relative to the midday circles for the periods free of SO_2 precipitation and pollution.

established in the remote marine CBL (Davis et al., 1999), the demonstration of the details of the formation of Aitken nuclei from this gas phase processing remain incomplete because of the difficulty of the measurements within the CBL, although evidence for the formation of particles of a few nanometers diameter has been demonstrated (Weber et al., 2001).

The increases in CCN concentrations at 0.2 % to 0.6 % supersaturation during SU2 and SC2 circles compared to earlier are consistent with the PCASP probe spectra. Aerosols for diameters of 0.14 to 0.185 µm had concentrations twice as great as the earlier circles (Fig. 4). Accumulation mode aerosols are primarily ammonium sulfate in the remote marine CBL as deduced from volatility measurements. The PCASP spectra showed no significant change for sizes >0.5 µm between the early and later CBL circles (Fig. 4). These larger sized aerosols are typically dominated by sea salt. The production of sea salt aerosols is well known to be a strong function of surface wind speed. With wind speeds of 12 to 15 m s^{-1} during all CBL circles (the highest during the RICO flights), the number concentrations of salt aerosols generated from sea spray would be expected to be similar throughout the day. Sea spray derived salt aerosols would produce CCN that activated at the lowest supersaturations ($\leq$0.1 %), which corresponded to sizes >0.1 µm diameter based on the in flight calibration. However, CCN concentrations that activated at <0.1 % were generally lower in the later circles compared to earlier with SC2 circle affected the most (Fig. 6 inset).

3.3 SO_2 and CCN correlations

In two periods during RF14 there were linear correlations of SO_2 with CCN and of CN with CCN over a wide range of concentrations and supersaturations. While the latter correlation is expected, the former has not previously been observed in the marine atmosphere with a time resolution of the SO_2 measurements much greater than for CCN measurements. Furthermore, the correlations between SO_2 and CCN increased as the supersaturation increased.

For the period of the SU1 circle most impacted by ship exhaust (400 to 500 s of Figs. 1, 4), SO_2 ranged from 50 to 600 pptv with concomitant changes in CN and CCN. SO_2 and CCN were linearly correlated at all supersaturations (Fig. 7; Table 4), although the correlation coefficients decreased slightly with supersaturations <0.2 %. There were similar correlations between CN and CCN for this period (Table 4).

For the SU1 case, the production of SO_2 and primary sulfate aerosols in the combustion process would be responsible for the correlation of SO_2 and CCN over the wide range of supersaturations. During combustion oxidation of SO_2 to sulfuric acid and adsorption of SO_2 and sulfuric acid on to soot particles would form externally mixed aerosols that would have a strong influence on the larger CCN with supersaturations $\leq$0.1 %. Addition of SO_2 and sulfuric acid to salt aerosols would also contribute the correlations with the larger CCN with supersaturations $\leq$0.1 %. Downwind of the source a large number of small aerosols could be produced by further oxidation of SO_2 through homogeneous reactions to sulfuric acid and heterogeneous reactions in aerosols by H_2O_2, which would be aided by neutralization from gas phase ammonia and acidity reductions by hydrochloric acid evaporation from salt aerosols.

During the SU2 circle (1100 to 1500 of, Figs. 1, 4) SO_2, CN, and CCN also displayed a synchronous variation in their concentrations. Although the variation in SO_2 was only 15 to 45 pptv, there was enough of a perturbation to assess the correlation of these three constituents. For CCN activated at 1.5 % supersaturation there was a linear correlation between SO_2 and CCN (Fig. 7; Table 4) with statistically the same slope as for the pollution case. For the intermediate supersaturations of 0.2 to 0.6 % the correlation increased as the supersaturation increased (Fig. 7). There was no linear correlation between SO_2 and CCN activated at supersaturations $\leq$0.1 % (Fig. 7; Table 4). The linear correlations of CN and CCN were similar to those of SO_2 and CCN (Table 4).

With the absence of soot particles and primary sulfates from combustion during the SU2 circle, the very low SO_2 concentrations would not be sufficient to affect the CCN that activate at supersaturations $\leq$0.1 % as in the pollution plume. The CCN concentrations activated at $\leq$0.1 % supersaturation were similar throughout the day for all the CBL circles (Fig. 6). If these low supersaturation CCN were sea salt, the diameters would have been in the range of 0.1 to 0.3 µm based on the in-flight calibration of the CCN spectrometer. These larger CCN of primarily sea salt would be uncorrelated to SO_2.

Table 4. Linear regressions of CCN (# cm^{-3}) on SO_2 (pptv) or CN (# cm^{-3}) for two CBL events. SU1: Period 395 to 475 s for a pollution event ($n = 24$). SU2: Period 1200 to 1500 s in the absence of pollution ($n = 65$).

	SO_2				CN			
	SU1 395 to 475 s		SU2 1200 to 1500 s		SU1 395 to 475 s		SU2 1200 to 1500 s	
Supersaturation	1.5 %	0.1 %	1.5 %	0.1 %	1.5 %	0.1 %	1.5 %	0.1 %
Slope	1.35	0.73	1.69	0.081	0.60	0.31	0.61	0.06
Std. dev of slope	0.08	0.08	0.29	0.21	0.05	0.05	0.11	0.08
Correlation coeff.	0.96	0.89	0.59	0.048	0.92	0.82	0.58	0.10

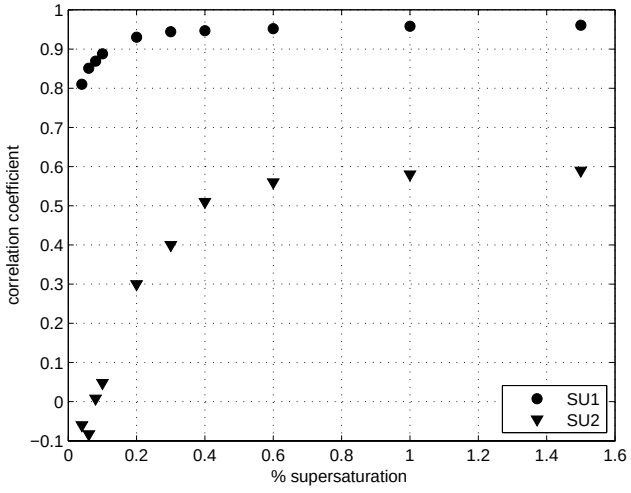

Fig. 7. Correlation coefficients for linear regressions of CCN number concentrations at various supersaturations on SO_2 concentrations. SU1: a pollution plume from 400 s to 500 s of circle at 90 m. SU2: for the period 1200 s to 1500 s of the circle at 90 m in the absence of pollution.

The increasing correlation between SO_2 and CCN activating at $\geq$0.2 % supersaturation (Fig. 7) could be the result of SO_2 conversion to sulfate or SO_2 uptake by existing small CCN or by pre-CCN Aitken aerosols which were activated by reaction with SO_2. The CCN concentrations at supersaturations $>$0.1 % in the late CBL circles provided more than half of the total number of CCN (Fig. 5) with a leveling off at 0.6 % supersaturation.

The source of the increased CCN may not be solely in the CBL. Ozone covaried with SO_2, CN, and CCN for this period on SU2, although with a lag time of unknown origin. Because O_3 is destroyed in the CBL, the O_3 increases must have been from above the CBL. Water vapor MR and DMS were anticorrelated to the changes in SO_2, O_3, CCN, and CN for this period. Increases in DMS and water vapor MR indicated updrafts from very near the surface. Decreases in water vapor MR indicated that the air parcels would have come from cooler, drier air above. Lower DMS concentrations also indicated entrainment of air from the cloud layer of the trade wind where DMS concentrations are typically lower than the CBL (Conley et al., 2009; Davis et al., 1999; Russell et al., 1998). At the time of the these measurements (Table 1) the solar zenith angle was $>$80°, which makes homogeneous oxidation of DMS to SO_2 initiated by hydroxyl radical negligible.

The sum of these measurements points toward subsidence of air parcels from the entrainment zone between the top of the CBL and the cloud base. For this period SU2 only cumulus congestus clouds were visible on the forward video of the aircraft. The peaks in the DMS and water vapor concentrations corresponded to the time periods when clouds were directly overhead as indicated by the upward viewing infrared radiometer. Updrafts related to these clouds must have been responsible for the upward flux of DMS and water vapor. SO_2 concentrations $\leq$20 pptv (near 1180 s and after 1500 s of SU2 in Fig. 1) occurred where many small non-precipitating clouds were overhead. Conversely, the peaks in SO_2, CCN, and CN concentrations occurred when there were no clouds overhead. Entrainment of SO_2, CCN, and CN appeared to be responsible for the observed increases.

4 Conclusions

Correlations between SO_2 and CCN at supersaturations $>$0.2 % in the CBL were found which are consistent with SO_2 being a primary source of the smallest CCN. In the absence of a pollution source of SO_2 CCN were only correlated with SO_2 at supersaturations above 0.2 % with strongest correlations $\geq$0.6 % supersaturation. Evidence of entrainment of CCN from the cloud layer into the CBL was found in precipitation free regions near sunset.

The concentrations of CCN at supersaturations $>$0.2 % and aerosols with diameters $<$0.2 µm were markedly higher in the late afternoon compared to the midday period. The difference appeared to be related the occurrence of precipitation during the midday even when comparing precipitation free regions for the two CBL sampling periods. Because

the concentrations of CCN at supersaturations $\leq$0.1 % were similar for both periods and the concentrations of CCN at supersaturations of 0.2 % to 0.6 % were much lower during the midday period, CCN supersaturations of 0.2 % to 0.6 % appeared to have a greater role in formation of clouds that precipitate. Hudson and Noble (2009) found that cloud drop concentrations were well correlated to CCN activated at 1 % supersaturation for the surface flight levels. The mean effective supersaturation for the surface circles during RICO was 0.5 % with a range of 0.2–1.5 % supersaturation. This is similar to the range found for stratocumulus cloud decks with mean CCN that activate at 1 % supersaturation (Hudson et al., 2010).

Acknowledgements. Support from the National Science Foundation under grants ATM-0342138, ATM-0627227, ATM-0627227, and ATM-0342618 is gratefully acknowledged. National Center for Atmospheric Research (NCAR) is sponsored by the National Science Foundation. We thank the NCAR Research Aviation Facility for their assistance throughout the C-130 operation phase of RICO. Data from the RICO project archive at NCAR Earth Observing Laboratory archive for the C-130 and the Radar Image Archive for the radar images for RF14 are gratefully acknowledged.

Edited by: R. Krejci

References

Arthur, D. K., Lasher-Trapp, S., Abdel-Haleem, A., Klosterman, N., and Ebert, D. S.: A new three-dimensional visualization system for combining aircraft and radar data and its application to RICO observations, J. Atmos. Oceanic Tech., 27, 811–828, doi:10.1175/2009JTECHA1395.1, 2010.

Bandy, A. R., Thornton, D. C., and Driedger, A. R.: Airborne measurements of sulfur dioxide, dimethyl sulfide, carbon disulfide, and carbonyl sulfide by isotope dilution gas chromatography mass spectrometry, J. Geophys. Res.-Atmos., 98, 23423–23433, 1993.

Bandy, A. R., Thornton, D. C., Blomquist, B. W., Chen, S., Wade, T. P., Ianni, J. C., Mitchell, G. M., and Nadler, W.: Chemistry of dimethyl sulfide in the equatorial Pacific atmosphere, Geophys. Res. Lett., 23, 741–744, 1996.

Capaldo, K., Corbett, J. J., Kasibhatla, P., Fischbeck, P., and Pandis, S. N.: Effects of ship emissions on sulphur cycling and radiative climate forcing over the ocean, Nature, 400, 743–746, 1999.

Colon-Robles, M., Rauber, R. M., and Jensen, J. B.: Influence of low-level wind speed on droplet spectra near cloud base in trade wind cumulus, Geophys. Res. Lett., 33, L20814, doi:10.1029/2006GL027487, 2006.

Conley, S. A., Faloona, I., Miller, G. H., Lenschow, D. H., Blomquist, B., and Bandy, A.: Closing the dimethyl sulfide budget in the tropical marine boundary layer during the Pacific Atmospheric Sulfur Experiment, Atmos. Chem. Phys., 9, 8745–8756, doi:10.5194/acp-9-8745-2009, 2009.

Davis, D., G., C., Bandy, A., Thornton, D., Eisele, F., Mauldin, L., Tanner, D., Lenschow, D., Fuelberg, H., Huebert, B., Heath, J., Clarke, A., and Blake, D.: Dimethyl sulfide oxidation in the equatorial Pacific: comparison of model simulations with field observations for DMS, SO_2, H_2SO_4(g), MSA(g), MS and NSS, J. Geophys. Res.-Atmos., 104, 5765–5784, 1999.

Gerber, H. E., Frick, G. M., Jensen, J. B., and Hudson, J. G.: Entrainment, mixing, and microphysics in trade-wind cumulus, J. Meteorol. Soc. Jpn., 86, 87–106, 2008.

Hudson, J. G. and Mishra, S.: Relationships between CCN and cloud microphysics variations in clean maritime air, Geophys. Res. Lett., 34, L16804, doi:10.1029/2007GL030044, 2007.

Hudson, J. G. and Noble, S.: CCN and cloud droplet concentrations at a remote ocean site, Geophys. Res. Lett., 36, L13812, doi:10.1029/2009gl038465, 2009.

Hudson, J. G., Noble, S., and Jha, V.: Stratus cloud supersaturations, Geophys. Res. Lett., 37, L21813, doi:10.1029/2010gl045197, 2010.

Hudson, J. G., Jha, V., and Noble, S.: Drizzle correlations with giant nuclei, Geophys. Res. Lett., 38, L05808 doi:10.1029/2010gl046207, 2011.

Lowenstein, J. H., Blyth, A. M., and Lawson, R. P.: Early evolution of the largest-sized droplets in maritime cumulus clouds, Q. J. Roy. Meteor. Soc., 136, 708–717, doi:10.1002/qj.597, 2010.

Rauber, R. M., Stevens, B., Ochs, H. T., Knight, C., Albrecht, B. A., Blyth, A. M., Fairall, C. W., Jensen, J. B., Lasher-Trapp, S. G., Mayol-Bracero, O. L., Vali, G., Anderson, J. R., Baker, B. A., Bandy, A. R., Burnet, E., Brenguier, J. L., Brewer, W. A., Brown, P. R. A., Chuang, P., Cotton, W. R., Di Girolamo, L. D., Geerts, B., Gerber, H., Goke, S., Gomes, L., Heikes, B. G., Hudson, J. G., Kollias, P., Lawson, R. P., Krueger, S. K., Lenschow, D. H., Nuijens, L., O'Sullivan, D. W., Rilling, R. A., Rogers, D. C., Siebesma, A. P., Snodgrass, E., Stith, J. L., Thornton, D. C., Tucker, S., Twohy, C. H., and Zuidema, P.: Electronic supplement to Rain in (shallow) Cumulus over the Ocean – The RICO campaign, B. Am. Meteorol. Soc., 88, S12–S18, 2007a.

Rauber, R. M., Stevens, B., Ochs, H. T., Knight, C., Albrecht, B. A., Blyth, A. M., Fairall, C. W., Jensen, J. B., Lasher-Trapp, S. G., Mayol-Bracero, O. L., Vali, G., Anderson, J. R., Baker, B. A., Bandy, A. R., Burnet, E., Brenguier, J. L., Brewer, W. A., Brown, P. R. A., Chuang, P., Cotton, W. R., Di Girolamo, L. D., Geerts, B., Gerber, H., Goke, S., Gomes, L., Heikes, B. G., Hudson, J. G., Kollias, P., Lawson, R. P., Krueger, S. K., Lenschow, D. H., Nuijens, L., O'Sullivan, D. W., Rilling, R. A., Rogers, D. C., Siebesma, A. P., Snodgrass, E., Stith, J. L., Thornton, D. C., Tucker, S., Twohy, C. H., and Zuidema, P.: Rain in shallow cumulus over the ocean - The RICO campaign, B. Am. Meteorol. Soc., 88, 1912–1928, 2007b.

Reiche, C. H. and Lasher-Trapp, S.: The minor importance of giant aerosol to precipitation development within small trade wind cumuli observed during RICO, Atmos. Res., 95, 386–399, 2010.

Russell, L. M., Lenschow, D. H., Laursen, K. K., Krummel, P. B., Siems, S. T., Bandy, A. R., Thornton, D. C., and Bates, T. S.: Bidirectional mixing in an ACE 1 marine boundary layer overlain by a second turbulent layer, J. Geophys. Res.-Atmos., 103, 16411–16432, doi:10.1029/97jd03437, 1998.

Snodgrass, E. R., Di Girolamo, L., and Rauber, R. M.: Precipitation characteristics of trade wind clouds during RICO derived from radar, satellite, and aircraft measurements, J. Appl. Meteorol. Climatol., 48, 464–483, 2009.

Thornton, D. C., Bandy, A. R., Beltz, N., Driedger, A. R., and Ferek, R.: Advection of sulfur dioxide over the western Atlantic Ocean during CITE-3, J. Geophys. Res.-Atmos., 98, 23459–

23467, 1993.

Thornton, D., Bandy, A., Blomquist, B., Driedger, A., and Wade, T.: Sulfur dioxide distribution over the Pacific Ocean 1991–1996, J. Geophys. Res.-Atmos., 104, 5845–5854, 1999.

Thornton, D., Bandy, A., Tu, F., Blomquist, B., Mitchell, G., Nadler, W., and Lenschow, D.: Fast airborne sulfur dioxide measurements by atmospheric pressure ionization mass spectrometry (APIMS), J. Geophys. Res.-Atmos., 107, 4632 doi:10.1029/2002JD002289, 2002.

Tu, F. H., Thornton, D. C., Bandy, A. R., Carmichael, G. R., Tang, Y., Thornhill, K. L., Sachse, G. W., and Blake, D. R.: Long-range transport of sulfur dioxide in the central Pacific, J. Geophys. Res.-Atmos., 109, D15S08, doi:10.1029/2003JD004309, 2004.

Weber, R. J., Chen, G., Davis, D. D., Mauldin, R. L., Tanner, D. J., Eisele, F. L., Clarke, A. D., Thornton, D. C., and Bandy, A. R.: Measurements of enhanced H2SO4 and 3-4 nm particles near a frontal cloud during the First Aerosol Characterization Experiment (ACE 1), J. Geophys. Res. Atmos., 106, 24107–24117, 2001.